ELSEVIER

Journal of Nuclear Materials 283–287 (2000) 574–578

journal of nuclear materials

www.elsevier.nl/locate/jnucmat

Mechanical and thermal properties of 2D and 3D SiC/SiC composites

R. Yamada *, T. Taguchi, N. Igawa

Department of Materials Science, Japan Atomic Energy Research Institute, Tokai-mura, Ibaraki-ken 319-1195, Japan

Abstract

SiC fiber-reinforced SiC composites (SiC/SiC), whose preforms had 3D satin weave or 2D non-woven fabric, were fabricated by chemical vapor infiltration (CVI) or polymer impregnation and pyrolysis (PIP). The 3D satin texture made from Hi-Nicalon Type S fiber was successfully woven although the fiber has high elastic modulus. Both CVI and PIP SiC/SiC composites of Type S fiber had higher thermal conductivity than those of Hi-Nicalon fiber. These results can be ascribed to higher thermal conductivity of Type S fiber. The thermal conductivity of the 3D PIP SiC/SiC composites was increased after annealing at 1400°C in vacuum. The bend strength of the 2D CVI SiC/SiC composites of non-coated Hi-Nicalon fiber was higher than that of non-coated Type S fiber, indicating that interfacial modification for Type S fiber is needed to obtain good mechanical properties.

1. Introduction

From their attractive low-radioactivity and high-temperature properties, SiC fiber-reinforced SiC composites (SiC/SiC) have the high economic, safety and environmental potential for an advanced structural material of fusion reactors. Conceptual design studies of such reactors, for instance, ARIES-I [1] and DREAM [2], have been conducted under certain values for mechanical and thermal properties of SiC/SiC composites that define allowable limits of stresses and temperatures for first walls. In order to satisfy the specifications of the design studies, the high performance of SiC/SiC composites should be pursued since their properties experience degradation during neutron irradiation. Improvement in mechanical and thermal properties of SiC/SiC composites is still needed by means of optimizing fabrication processes, such as chemical vapor infiltration (CVI), polymer impregnation and pyrolysis (PIP), and reaction bonding (RB).

In order to develop SiC/SiC composites that are robust under 3D stress distribution in fusion reactors, we employed preforms of 3D weave or 2D non-woven fabric for the composites. The non-woven fabric was made from chopped yarns of which the fiber length was long enough to give a partial 3D fiber-configuration. We will report the results of the measurements of mechanical and thermal properties of CVI and PIP SiC/SiC composites made from these preforms.

2. Materials

The 3D satin weave and 2D non-woven fabric were made from the yarn of Hi-Nicalon fiber [3,4] or recently developed Hi-Nicalon Type S fiber (Type S) [5–7]. Each yarn consisted of 500 filaments. The fibers used here had no interfacial coating.

In the case of 3D satin weave, two kinds of textures were woven by Shikibou Ltd. Japan, namely the fiber configuration ratios were $X:Y:Z = 1:1:0.1$ and $1:1:0.2$. Applying the technique developed in Si–Ti–C–O fiber(Tyranno LoxM fiber), Kawasaki Heavy Industries Ltd. Japan synthesized these Nicalon-based preforms to PIP SiC/SiC composites [8,9]. Prior to PIP, the preforms were coated with about 2 μm CVI SiC. The PIP was repeated six cycles using polycarbosilane as the polymer and pyrolyzing it at 1000°C. The fabricated composites were machined to plates with a nominal thickness of

* Corresponding author. Tel.: +81-29 282 5403; fax: +81-29 282 6556.

E-mail address: reiji@popsvr.tokai.jaeri.go.jp (R. Yamada).

0022-3115/00/$ - see front matter
PII: S0022-3115(00)00144-6

3 mm. The fiber volume factions were 26–28% for prepared samples.

For non-woven fabric, the chopped yarn mats were employed and synthesized to CVI SiC/SiC composites by Mitsui Engineering & Shipbuilding Co., Ltd. Japan [10]. Several mats made from 25 mm-long chopped yarns were piled to make a preform of 4–5 mm thickness for CVI. In this study 2D piled mats were used, but complex shapes of mat would be possible for future fusion applications. Since chopped yarns are 3D tangled in the mats, these composites are expected to be to some extent durable under 3D stresses. The fabricated composites were machined to plates with a nominal thickness of 3 mm. The fiber volume factions were about 35% for Hi-Nicalon and 30% for Type S composites.

3. Experimental

Thermal diffusivity of SiC/SiC composites was measured in the temperature range of 15–1200°C in vacuum using laser flash method. Thermal diffusivity, α, was obtained by $t_{1/2}$ method using the following equation: $\alpha = 1.388L^2/t_{1/2}$, where $t_{1/2}$ is the time required reaching half of the total temperature rise on the rear surface of a specimen, and L is the specimen thickness. Thermal conductivity, λ, is given by the following equation: $\lambda = \alpha C_p \rho$, where C_p and ρ are the specific heat and the sample density, respectively. In the present work, specific heat of SiC/SiC composites was assumed to be the same as that of monolithic SiC obtained from the literature [11]. The size of specimens for thermal diffusivity was 3 mm in thickness and 10 mm in diameter.

Room-temperature strengths were determined by a three-point bend fixture that had a span of 20 mm. The strengths were evaluated by the equation of $3FL/2WT^2$, where F is the load, L the span length, and W and T are the width and the thickness of specimen, respectively. The loading rate was 0.1 mm/min. Specimens for bend tests were cut, and then machined by a surface grinder using diamond grindstones of No. 100 and 800, and finally buffing. Typical specimen dimensions were 3 mm in thickness, 4 mm in width and 25 mm in length.

4. Results and discussion

4.1. Mechanical properties

Fig. 1 exhibits 3D textures successfully woven with Type S fiber, even though it has a very high elastic modulus of 420 GPa compared to 270 GPa for Hi-Nicalon fiber [6]. In order to study the effect of Z-configuration of Type S fiber, we prepared two types of textures, namely $X{:}Y{:}Z = 1{:}1{:}0.1$ and 1:1:0.2. Fig. 2 shows typical surface features and cracking patterns of specimens after bend tests for 2D non-woven mat-type CVI SiC/SiC and 3D satin-type PIP SiC/SiC composites.

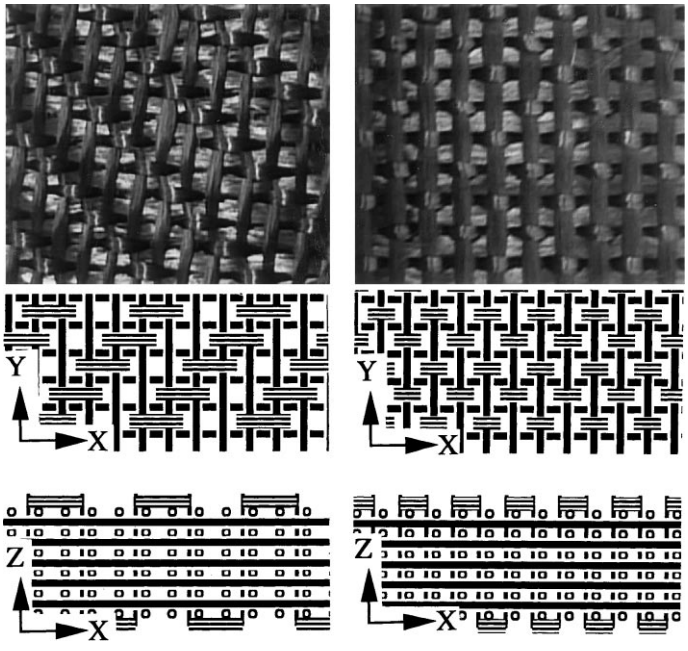

Fig. 1. 3D textures woven with Hi-Nicalon Type S fiber. The ratios of yarn configuration in a fabric, $X{:}Y{:}Z$, are1:1:0.1 for the left-hand side, and 1:1:0.2 for the right-hand side. The schematic illustrations show the features of textile for X–Y and X–Z surfaces.

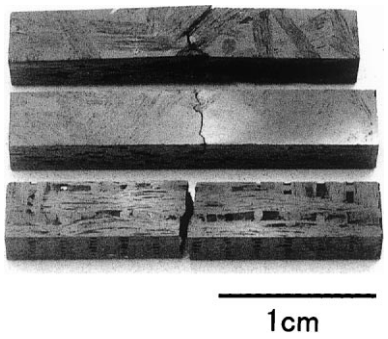

Fig. 2. Photographs of SiC/SiC specimens after bend tests: 2D non-woven fabric CVI SiC/SiC of Hi-Nicalon fiber (upper) and of Hi-Nicalon Type S fiber (middle), and 3D satin PIP SiC/SiC of Hi-Nicalon Type S fiber (bottom).

In the figure, the chopped yarns and the continuously woven yarns can be seen in the 2D CVI and 3D PIP specimens, respectively.

The bend tests were carried out for three specimens or more in each composite. Fig. 3 shows some of the results of bend strength–displacement curves for the above specimens. The averaged flexural strength and its standard deviation as well as fracture energy derived from the area integration of bend strength–displacement curves are shown in Table 1. The 2D non-woven fabric CVI SiC/SiC of Hi-Nicalon fiber had the highest flexural strength among samples used in this study. The reason why there is strong difference in strength between the composites of Hi-Nicalon and Type S fiber may be explained from the fact that the interface between Hi-Nicalon fiber and the matrix is different from that between Type S fiber and the matrix. As shown in Fig. 4,

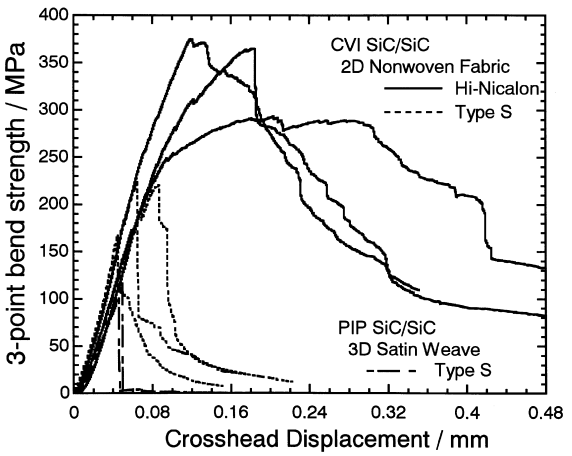

Fig. 3. Bend strength vs crosshead displacement curves for 2D non-woven fabric CVI SiC/SiC composites of Hi-Nicalon (solid) and of Hi-Nicalon Type S (dot), and 3D satin PIP SiC/SiC composites of Hi-Nicalon Type S (dot and dash).

the cross-sectional views of the 2D CVI SiC/SiC composites reveal that the interface of the Hi-Nicalon fiber is more prominent than that of the Type S fiber, which suggest the former interface is thicker than the latter one. It has been reported that graphitic carbon first appeared in the order of 10 nm on the SiC surface of a fiber at the initial stage of CVI SiC [12]. In addition, since Hi-Nicalon fiber has originally carbon-rich concentration [6], the surface region of fiber may be altered to thin carbon layer during heating for CVI, whereas Type S fiber, which has near stoichiometric Si/C concentration, cannot expect such effect. The appropriate thickness of carbon layer is known to increase bend strength and toughness [13]. The non-catastrophic failure of the Hi-Nicalon non-woven composites can, therefore, be ascribed to thin carbon layer unintentionally formed on chopped yarns. As mentioned in Section 2, carbon coating was not done to all fibers used here. This study indicates that surface modification including carbon coating on Type S fiber is needed to improve the mechanical properties of the composites.

4.2. Thermal properties

Figs. 5 and 6 show the results of thermal conductivity for 2D non-woven fabric CVI and 3D satin PIP SiC/SiC composites using Hi-Nicalon fiber or Type S fiber. These values were obtained by measuring the thermal diffusivity through the thickness, namely Z-direction. In the case of the 2D CVI SiC/SiC composites, an increase of 15–20% in thermal conductivity was observed in the whole temperature range when Type S fiber was employed. It is reported that thermal conductivity of Hi-Nicalon Type S fiber at 25°C and 500°C were 18.4 and 16.3 W/mK, respectively, which are higher than those of Hi-Nicalon [7]. Even for the mat-type SiC/SiC composites, some portion of chopped Type S yarns, which were configured to Z-direction, could contribute to increase the thermal conductivity. In the case of the 3D PIP SiC/SiC composites, a similar tendency was observed. The composites of Type S exhibited 30–60% higher thermal conductivity compared to the Hi-Nicalon ones in the case of the fiber configuration, $X{:}Y{:}Z = 1{:}1{:}0.2$. It should be noted that the thermal conductivity of the Type S composites increased when the Z configuration ratio increased from 0.1 to 0.2. It may not be difficult to increase the ratio up to $X{:}Y{:}Z = 1{:}1{:}1$ or more, which would achieve much higher through-the-thickness thermal conductivity. Concerning non-annealed specimens in Fig. 6, the thermal diffusivity decreased with increasing temperature due to phonon scattering, whereas the temperature dependence of the thermal conductivity was strongly affected by that of specific heat of SiC.

As shown in Fig. 6, the thermal conductivity of the PIP SiC/SiC composites whose pyrolysis temperature

Table 1
Flexural strength and its standard deviation, and fracture energy of SiC/SiC composites

Specimen	Flexural strength (MPa)	Fracture energy (kJ/m^2)
2D non-woven fabric CVI (Hi-Nicalon)	345 ± 45	~5.2
2D non-woven fabric CVI (Hi-Nicalon Type S)	193 ± 35	~0.5
3D satin weave PIP (Hi-Nicalon Type S)	109 ± 7	~0.1

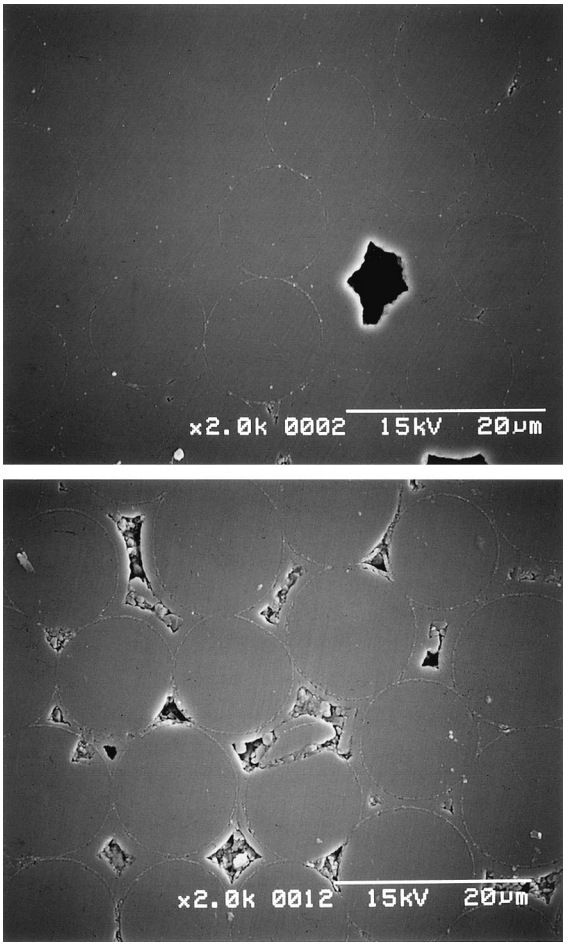

Fig. 4. SEM micrographs of cross-sectioned 2D non-woven fabric CVI SiC/SiC composites of Hi-Nicalon Type S (top) and of Hi-Nicalon (bottom).

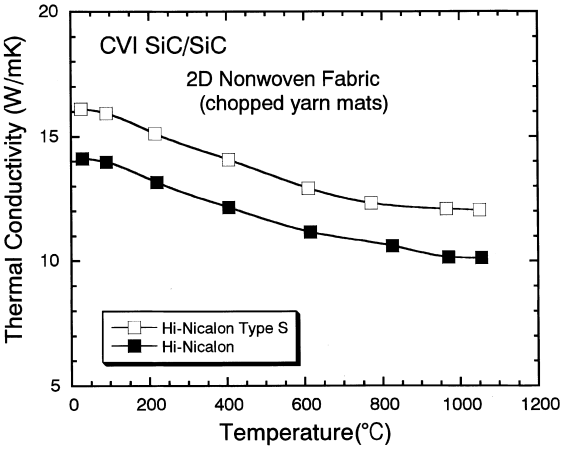

Fig. 5. Comparison of thermal conductivity of 2D non-woven fabric CVI SiC/SiC composites when Hi-Nicalon fiber and Hi-Nicalon Type S fiber was used.

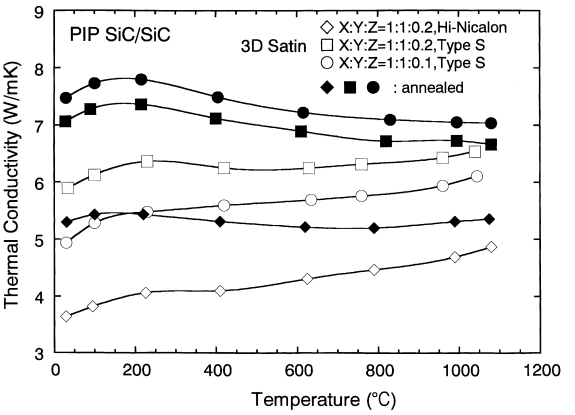

Fig. 6. Comparison of thermal conductivity of 3D satin weave PIP SiC/SiC composites when Hi-Nicalon and Hi-Nicalon Type S was used. Also compared between annealed and non-annealed case. The annealing condition was 10 h at 1400°C in vacuum. The conditions of 3D preforms were as follows: Hi-Nicalon and $X:Y:Z = 1:1:0.2$ (◇, ◆), Hi-Nicalon Type S and $X:Y:Z = 1:1:0.1$ (○, ●), Hi-Nicalon Type S and $X:Y:Z = 1:1:0.2$ (□, ■), where white and black symbols represent non-annealed and annealed specimens, respectively.

was 1000°C was increased by annealing them at 1400°C in vacuum. We have already reported that the annealing at a temperature higher than pyrolysis temperature led an increase in thermal conductivity due to the growth of SiC crystallite size [14]. A similar phenomenon took place in the present PIP SiC/SiC composites, although it is not clear that the thermal conductivity of the Hi-Nicalon Type S annealed composite for the $X:Y:Z = 1:1:0.1$ became slightly higher than that for $X:Y:Z = 1:1:0.2$.

5. Summary and conclusions

The bend strength and thermal diffusivity measurements were carried out for 3D satin weave PIP and 2D

non-woven fabric CVI SiC/SiC composites. Both CVI and PIP SiC/SiC composites showed higher through-the-thickness thermal conductivity for Hi-Nicalon Type S than for Hi-Nicalon. In the case of 3D weave, the thermal conductivity increased when the ratio of Type S fiber configured to Z-direction increased. These results can be ascribed to higher thermal conductivity of Type S fiber. It was observed that annealing in vacuum had a positive effect on thermal conductivity of PIP SiC/SiC due to the growth of SiC crystallite size, when pyrolysis temperature was less than annealing temperature. The CVI SiC/SiC composites of Hi-Nicalon fiber exhibited better mechanical properties compared to those of Hi-Nicalon Type S fiber. It indicates that the interfacial modification on fiber is needed to improve the properties when a stoichiometric fiber such as the Type S fiber is used. The present non-woven fabric CVI SiC/SiC composites exhibited relatively better performance in thermal and mechanical properties. This result is favorable for fusion applications if taking account a partial 3D-fiber configuration of the non-woven fabric as well as relatively easy fabrication of complex shapes compared with 3D weaves. It was shown that Hi-Nicalon Type S fiber that has very high elastic modulus could be three-dimensionally woven. This result would expand the field of applications for Hi-Nicalon Type S fiber.

References

[1] S. Sharafat, C.P.C. Wong, E.E. Reis, Fus. Technol. 19 (1991) 901.
[2] S. Ueda, S. Nishio, Y. Seki, R. Kurihara, J. Adachi, S. Yamazaki, J. Nucl. Mater. 258 (1998) 1589.
[3] K. Okamura, M. Sato, T. Seguchi, S. Kawanishi, in: Proceedings of the First Japanese International SAME Symposium, 1989, p. 929.
[4] M. Takeda, J. Sakamoto, Y. Imai, H. Ichikawa, T. Ishikawa, Ceram. Eng. Sci. Proc. 15 (4) (1994) 133.
[5] M. Takeda, J. Sakamoto, A. Saeki, Y. Imai, H. Ichikawa, Ceram. Eng. Sci. Proc. 16 (4&5) (1995) 37.
[6] M. Takeda, A. Urano, J. Sakamoto, Y. Imai, J. Nucl. Mater. 258–263 (1998) 1594.
[7] A. Urano, J. Sakamoto, M. Takeda, Y. Imai, H. Araki, T. Noda, Ceram. Eng. Sci. Proc. 19 (3) (1998) 55.
[8] K. Nishio, K. Igashira, S. Okazaki, in: Proceedings of the Fifth Japanese International SAMPE Symposium, 1997, p. 1159.
[9] K. Igashira, K. Nishio, T. Suemitsu, in: Proceedings of the European Conference on Composite Materials Science, Technologies and Applications, ECCM-8, vol. 4, 1998, p. 39.
[10] K. Matsumoto, N. Fujioka, T. Hayakawa, N. Kawasaki, K. Sato, Key Engineering Materials, vol. 164&165, Trans-Tech, Aedermannsdorf, 1999, p. 49.
[11] M.W. Chase Jr., C.A. Davies, J.R. Downey Jr., D.F. Frurip, R.A. McDonald, A.N. Syverud, Journal of Physical and Chemical Reference Data 14 (Suppl. 1), JANAF Thermochemical Tables, 3rd Ed., Part 1, p. 634.
[12] H. Araki, T. Noda, F. Abe, H. Suzuki, J. Mater. Sci. Lett. 11 (1992) 1582.
[13] L.L. Snead, R.H. Jones, A. Kohayama, P. Fenici, J. Nucl. Mater. 233–237 (1996) 26.
[14] R. Yamada, T. Taguchi, J. Nakano, N. Igawa, Ceram. Eng. Sci. Proc. 20 (3) (1999) 273.